IEEE Access
Multidisciplinary | Rapid Review | Open Access Journal

Received 16 June 2022, accepted 29 June 2022, date of publication 7 July 2022, date of current version 18 July 2022.

Digital Object Identifier 10.1109/ACCESS.2022.3189348

RESEARCH ARTICLE

Optimal Solar Greenhouses Design Using Multiobjective Genetic Algorithm

BAHRAM MAHJOOB KARAMBASTI[1], MOHAMAD NAGHASHZADEGAN[1], MARYAM GHODRAT[2], GHADIR GHORBANI[3], ROY B. V. B. SIMORANGKIR[4], (Member, IEEE), AND ALI LALBAKHSH[5,6], (Senior Member, IEEE)

[1]Department of Mechanical Engineering, Faculty of Engineering, University of Guilan, Rasht 4199613776, Iran
[2]School of Engineering and Information Technology, University of New South Wales Canberra, Canberra, NSW 2052, Australia
[3]Department of Mechanical Engineering, Faculty of Engineering, Razi University, Kermanshah 6714414971, Iran
[4]Tyndall National Institute, University College Cork, Cork T12 R5CP, Ireland
[5]School of Engineering, Macquarie University, Sydney, NSW 2109, Australia
[6]School of Electrical and Data Engineering, University of Technology Sydney (UTS), Sydney, NSW 2007, Australia

Corresponding authors: Roy B. V. B. Simorangkir (roy.simorangkir@tyndall.ie) and Ali Lalbakhsh (ali.lalbakhsh@mq.edu.au)

ABSTRACT In greenhouse horticulture, solar energy is the key to extending the greenhouse using seasonal or daily thermal storage technology and decreasing the energy consumption rate, especially in subtropical climate areas. Therefore, the present research aims to reach the optimal physical parameters of common greenhouses in northern areas of Iran to harness the best possible amount of solar energy in a year. Three common types of greenhouses, including even-span, modified arch and Quonset types, are considered. Three-floor area sizes are investigated for each shape to find the optimal physical parameters based on each greenhouse size. A mathematical model is proposed that uses the total solar fraction to compute the radiation loss and the available hourly transmitted solar radiation inside the greenhouse. The best design parameters for each type and size of greenhouses are obtained through a multi-objective optimization technique to give maximum and minimum available solar energy in winter and summer. The results show that optimized greenhouses can capture sufficient solar radiation in cold months of a year for growing offseason vegetables in Rasht city. The optimal wall height and roof angle for an even-span greenhouse are found to be 3.8 m and 16°, respectively. The results also revealed that in a modified arch greenhouse, the ellipse aspect ratio for small and large sizes is 0.8 and for medium size is 0.25. For Quonset type, ellipse aspect ratio to width ratio for medium and large sizes is 0.6 and for small size is 0.8. The findings of the study showed that the Quonset greenhouse offers the highest performance compared to other greenhouses for the efficient use of solar energy throughout the year.

INDEX TERMS Solar radiation, greenhouse design, multi-objective optimization, genetic algorithm, total solar fraction.

NOMENCLATURE

A	Area (m^2)
DL	Length of day (hour)
F_t	Total solar fraction
G_{sc}	Extraterrestrial solar radiation
H	Height (m)
I_0	Extraterrestrial radiation on a horizontal plane (J/m^2)
I	Measured solar radiation on a horizontal plane (J/m^2)
I_b	Direct beam radiation (J/m^2)
I_d	Diffuse radiation (J/m^2)
I_g	Reflected radiation from the ground (J/m^2)
I_T	Hourly Solar radiation on an inclined plane (J/m^2)
k_T	The hourly clearness index
K	Extinction coefficient
L	Greenhouse cover thickness and length of the greenhouse (m)

The associate editor coordinating the review of this manuscript and approving it for publication was Mostafa M. Fouda.

S_c	Total solar radiation received by the cover (J)
S_{floor}	Transmitted solar radiation falling on the floor (J)
S_{ref}	Transmitted solar radiation reflected back to the greenhouse (J)
S_t	Solar radiation transmitted to the greenhouse (J)
S	Total solar radiation available inside the greenhouse (J)
$r_\perp$	Perpendicular component of unpolarized radiation
$r_\parallel$	Parallel component of unpolarized radiation
R_b	Fraction of the direct beam radiation on a sloped surface
R_d	Fraction of the diffuse radiation on a sloped surface
R_g	fraction of the reflected radiation from the ground
r	Radius
Z	Ellipse aspect ratio

GREEK LETTERS

θ	Angle of incidence
β	Angle of inclination
δ	Declination angle
ω	Hour angle
γ	Surface azimuth angle
ϕ	Latitude
ρ	Reflectance
ρ_a	Albedo ground
τ	Transmittance
τ_a	Absorption of radiation
n	refractive index and number of days

Subscripts

b	Direct beam radiation
d	Diffuse radiation
gr	Reflected from the ground radiation
rf	Refraction

I. INTRODUCTION

The increasing demand for energy and food as a result of rapid population growth is putting pressure on the resources that are used to provide these basic needs. Worsening is expected in the near future because of climate change and limited arable lands. Thus, efficient food production system has become a great concern to scientist in the world and the Food and Agriculture Organization of the United Nations (FAO) [1]. Greenhouse cultivation is a promising alternative to meet the increasing demand for food because of its higher production rate to the traditional farming. Nevertheless, greenhouse technology requires a high amount of energy for heating, cooling, and ventilation [2].

In order to overcome the huge energy consumption in greenhouse industry, exploitation of the sun thermal energy as the most accessible renewable energy sources has been a focus of many researchers in the recent years [3], [4]. In general, solar energy can be used in a greenhouse directly and indirectly by the help of additional equipment for energy conversion, converting the energy of sun to other types of energy. In addition, the sun is the key element in plant photosynthesis and also for illumination of the greenhouse. Main use of solar energy in greenhouse is for thermal heating in winters for off-season products. The greenhouse transparent cover allows the shortwave of solar radiation to transmit into the greenhouse but it is partially opaque to the long wave radiation which leads to the greenhouse effect. This process is in favor of plant growth in cold months or cold climates, increasing inside air temperature during a day is desirable for maximum crop production and can be obtained by keep the greenhouse envelope closed for the maximum use of solar radiation. However, in hot months or hot climates solar radiation has adverse effect and there is a need for cooling and ventilation in the greenhouse.

According to the aforementioned reasons, greenhouse design, orientation of placement, and the shape of the greenhouse are the most significant factors on the solar radiation gaining rate [5]. Thus, optimal design of solar greenhouses leads to the best use of solar energy and reducing the energy consumption in the greenhouse. It should be noted that besides the greenhouse structural design, several studies have been conducted on the usage of various passive energy systems in greenhouse cultivation such as phase change materials for heat storage, rapid temperature control for energy saving, water storage systems, utilization of Internet of Things (IoT) technologies for controlling temperature, and earth to air exchangers for heating and cooling [6]–[9]. Since the main focus of this study is the optimal design of various solar greenhouses, the existent literature regarding designing a greenhouse for the best use of the sun's thermal energy is reviewed in the following paragraphs.

Physical structure of solar greenhouses comprises of several components one of which is the material used for canopy cover. Optical properties of the cover have significant impact on the rate of solar radiation entering the greenhouse. In this regard, in an experimental research Chaysaz *et al.* [10] developed a power-heat cogeneration system using a photovoltaic-thermal hybrid collector (PV-T) in a small scale greenhouse in order to investigate the effect of various cover materials (glass, plastic, and polycarbonate) on the power and heat supply of the system. Piscia *et al.* [11] proposed a methodology based on the integration of energy simulation, CFD method and an optimization technique in order to optimize the greenhouse cover properties in night times for minimizing the heat loss by radiation. In a recent study, Mazzeo *et al.* [12] simulated a Venlo-type greenhouse with fixed floor area and volume in TRANSYS software to select the best type of glass for greenhouse cover in several locations in the world. Performance of the greenhouse for three types of glass (single, double, triple) with various thickness and properties were investigated.

Various aspects of designing the structure of solar greenhouses such as orientation, shape, style, and size of the greenhouse have been investigated in a number of studies. For example, Ghasemi Mobtaker *et al.* [13], [14], in two

papers, and Taki *et al.* [15] developed a dynamic thermal model to investigate the solar energy conversion and energy consumption in six common types of greenhouses in north west of Iran. They also simulate the thermal performance of a solar greenhouse and validate the results with an experimental study. Chen *et al.* [16] presented a mathematical model to calculate the global solar radiation captured in six greenhouses types in southern China, the best shape and orientation for capturing maximum solar radiation in winter is also selected. El-Maghlany *et al.* [17] developed a numerical method to investigate the transmitted solar radiation inside the elliptic shape greenhouses in different latitudes with tropical climate. In addition, Çakir *et al.* [18] studied the magnitude of solar radiation intercepted by the greenhouse cover for five greenhouses shapes, different dimensions and orientation are investigated for each shape and the greenhouse with the highest solar radiation gaining rate is introduced. Choab *et al.* [19] performed a study to examine the effect of greenhouse design parameters including the specification of cover material, shape and orientation of the greenhouse on the thermal performance and required energy for heating and cooling the greenhouse in Agadir Morocco. TRANSYS software was used for greenhouse modeling. In a review paper conducted by Choab *et al.* [20] the best greenhouse design parameters including shape, size, orientation, and cover materials for different latitudes and climates along with the various applications of solar energy in greenhouse industry were explored.

Hence, the greenhouse environment is an intricate dynamic system with uncertain features and enclosed with thin cover of transparent materials [21], [22]; the use of optimization techniques to achieve favorable conditions, including physical design variables and thermodynamic properties, is a promising method. To integrate optimization techniques in a greenhouse environment, much research has been focused on finding and improving the optimal conditions for a greenhouse where the efficient use of solar energy can be obtained. A combination of particle swarm optimization and genetic algorithm is developed by Chen *et al.* [22] to investigate the uncertain internal variables in the energy balance equation and predict the energy consumption in a greenhouse. More information on the basic and improved PSO algorithm can be found in Mellalou *et al.* [23] investigated the amount of transmitted solar energy inside two common shapes of greenhouses including even-span and uneven-span for various orientations and dimensions in Morocco, the volume of the greenhouses kept the same in the calculations and the best configurations of dimensions and orientations were presented for maximum amount of solar radiation at winter. In a recent research, Mahjoob Karambasti *et al.* [24] determined the optimal orientation and roof inclination angle of an even-span greenhouse with fixed floor area by employing a multi-objective optimization (MOGA) method and solar radiation distribution model for northern sections of Iran. It should be mentioned that apart from GA and PSO approaches, other nature-based and numerical algorithms, [25]–[37], such as gray wolf optimization, ant colony, neural networks and other types of natured based and numerical algorithms can be adopted for greenhouse optimal condition improvement.

From the literature review it can be deduced that most of the research conducted on the greenhouse physical structure are focused on maximizing the amount of solar radiation intercepted by the greenhouse in cold seasons. This approach leads to maximizing the amount of solar radiation in the greenhouse in hot seasons too which means increasing the energy usage for cooling and ventilation. Consequently, in summer months the use of greenhouse is not profitable and leads to decreasing the greenhouse cultivation calendar in a year especially in tropical areas such as northern sections of Iran. Moreover, research on the curved shape greenhouses are limited, in fact, to the best of our knowledge, there is no study investigated the effect of design parameters on the availability of solar radiation in a modified arch greenhouse. Last but not least, in many cases, the radiation loss from the transparent sections of the greenhouse is ignored or, in a few study, it limits to calculating the radiation loss from the north wall.

The discussed limitations are overcome by the model developed in this study, which aims at ascertaining the most efficient greenhouse physical parameters with the lowest heat load in winter and lowest cooling load in summer. For this reason, three most common greenhouse types, namely, even span, modified arch, and Quonset are considered and a solar radiation distribution model in the considered greenhouses is developed and integrated into a multi-objective optimization procedure to reach optimal physical parameters for each types of greenhouses. The objective of optimization is to maximize the magnitude the solar radiation available in the greenhouses in winter and minimize it in summer, so a maximization and minimization problem is obtained. Since greenhouses are built based on their land area, three different floor area sizes for each types of greenhouses are considered. A comprehensive anisotropic mathematical model is developed to calculate the hourly solar radiation inside the greenhouses. The model uses the total solar fraction to evaluate the radiation loss from all sections of each greenhouse and could cover all the possible shapes and orientations of the considered greenhouse types. Then, by employing a multi-objective optimization Genetic Algorithm (MOGA) the proposed model is optimized and optimal design parameters for each greenhouse are obtained. For each greenhouse type, three sets of optimal design parameters based on the size of the floor area are obtained, and the yearly performance of captured solar radiation for each solution is provided.

The main novelties of this study can be summarized as:

- Solar radiation available in the greenhouse is evaluated for various greenhouse types, structure and size for the first time in Iran.
- An anisotropic model in used for calculating the amount of solar radiation in the greenhouses.
- The total solar fraction is used for determining the radiation loss from the greenhouse for all the possible dimension and orientation.

- The optimal design parameters for each types of greenhouse are presented based on the size of the greenhouse.
- A novel method for integration of solar radiation distribution model with a multi-objective optimization process is presented.

II. THEORY AND MATHEMATICAL MODEL

Greenhouse cultivation is mainly used during off season traditional agriculture such as winter but this does not mean greenhouse should be used only in times that traditional agriculture is impossible like winter. In fact, greenhouse industry should be used for sustainable agricultural approaches. In Iran, there is a belief that greenhouse cultivation is only used in a few months in winter and autumn especially in areas with subtropical climate like Rasht. On the contrary, farmers should be capable of using greenhouses in other seasons in order to increase the production rate and enhance their productivity.

Solar radiation as a source of thermal energy decreases the energy consumption for heating the greenhouse in cold season. Conversely, in hot seasons, solar radiation causes greenhouse effect and increasing the inside temperature which needs a great deal of energy to keep the greenhouse environment in desirable condition. This leads to shorten the usage of greenhouse cultivation in year, especially in summer when the usage of greenhouse because of the high energy consumption is not economically viable.

Based on the climate conditions the time period for greenhouse cultivation varies in different location in the world, but as a general rule in the coldest and hottest time of the year greenhouses are not used for farming. Therefore, efficient use of solar energy in greenhouse can decrease the level of energy consumption in a year leads to extending the time of greenhouse cultivation. For the location of this study, Rasht (Iran) with subtropical climate, farmers do not use greenhouses in three months in summer including July, August, and September because of high temperature and also a few months in winter such as January, February, and March due to low temperature. This means that in almost half of the year greenhouse is out of service and causes farmers to be not intrigued for build and use greenhouses. The mean daily global solar irradiation intensity in Rasht according to the data given by Iran Meteorological Organization (IRIMO) in a cold winter day (February) and hot summer day (August) is $707 J/cm^2 day$ and $2130 J/cm^2 day$, respectively [38]. In this regard, two time periods in winter and summer, when the solar radiation intensity is in its lowest and highest, respectively, are considered to overcome the energy consumption challenge and for the maximum use of greenhouses throughout the year to the extent of a greenhouse physical structure possibility. These two time periods are 1st January to 30th February for winter and 1st June to 30th July for summer.

As it mentioned before this research is conducted for a case study in Rasht city located in the north of Iran with the geographical location of 37°28′ north latitude and 49°34′ east longitude. All meteorological data was obtained from IRIMO at the Agricultural Organization meteorological station in Rasht. Since wind is a common phenomenon in northern sections of Iran, curved shape greenhouses (modified arch and Quonset) are the most common types of greenhouses in this area because of their wind resistance. Therefore, modified arch and Quonset types along with the even-span type are selected in this study. For the mathematical modeling, MATLAB R2018b software is used to develop a script for three types of greenhouses to investigate the rate of solar radiation transmitted to the greenhouse on an hourly basis and determine the total solar radiation available in the greenhouse for a given day throughout a year. Therefore, in this study, a systematic and detailed approach is presented to analyze the available solar energy inside three common types of single-span greenhouses.

A. TYPE AND SPECIFICATIONS OF GREENHOUSES

Three common types of single-span greenhouses that are inused in northern Iran are shown in Figs. 1a-c: (a) even-span, (b) modified arch, and (c) Quonset. Among the presented types, the most commonly used shapes of greenhouses in Rasht are modified arch and Quonset types. As shown in Fig. 1, each type is divided into different inclined surfaces (wall and roofs). The south wall corresponds to the wall that is toward the south in the initial placement of the greenhouse. To select the best physical parameters for each type of greenhouse, calculations are performed for various greenhouse sizes, including small, medium and large greenhouses based on the floor area size. Floor areas for small, medium and large greenhouses are taken as 30m^2, 60m^2, and 120m^2, respectively. The physical parameters required for constructing each types of greenhouses and setting the orientation are taken as decision variables in the multi-objective optimization procedure. In order to consider all the possible orientations, it is assumed that the initial orientation of each greenhouse (zero degree) is along the E-W axis (east–west), and each greenhouse rotates in the clockwise direction from east to south to investigate the various azimuth angles (from 180° to −180°). Polyethylene sheets, with refractive index of 1.49, as one of the cheap and convenient material in Iran markets are considered for covering the greenhouse.

To assess all possible shapes for curved sections of the modified arch and Quonset types, the roof of the modified arch greenhouse and the whole shape of the Quonset greenhouse are considered as half elliptic cylinders. A cross-section of the elliptical part of these greenhouses is shown in Fig. 2.

In Fig. 2, the following geometrical relations in the polar coordinate for computing the radius r at the angle η based on the ellipse aspect ratio Z are presented:

$$r = \frac{Hr \times \frac{W}{2}}{\sqrt{(Hr \sin\eta)^2 + \left(\frac{W}{2}\cos\eta\right)^2}} = \frac{Hr}{\sqrt{(Z\cos\eta)^2 + \sin^2\eta}} \tag{1}$$

$$Z = \frac{2 \times Hr}{W}, \tag{2}$$

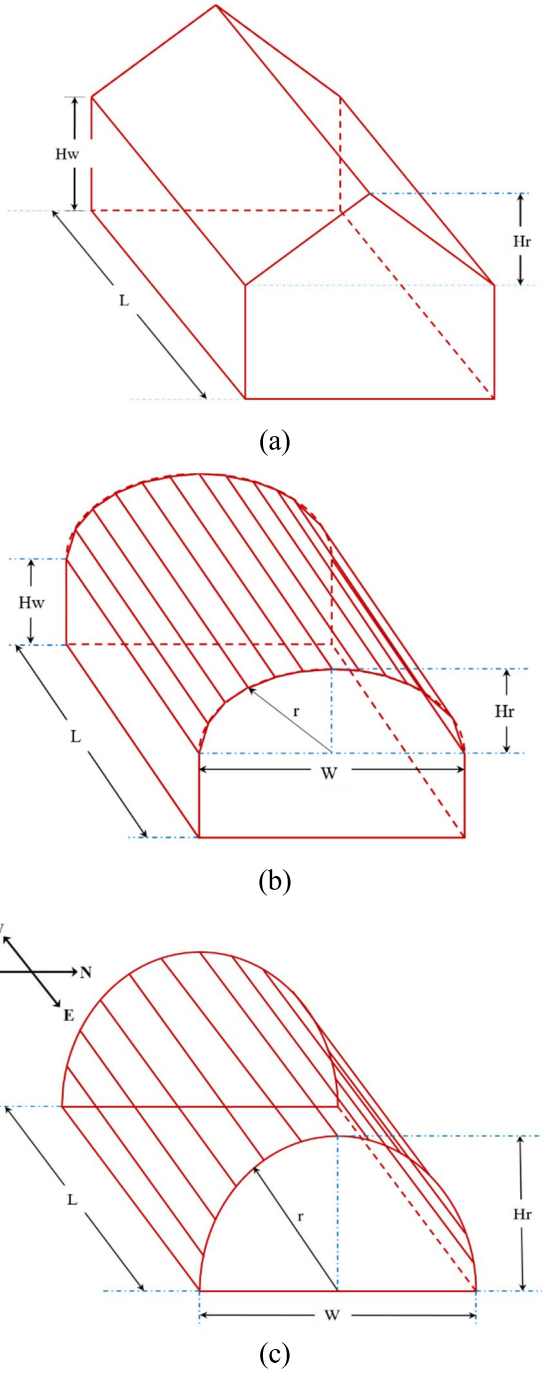

FIGURE 1. SW isometric view of the selected greenhouses at initial E-W orientation (zero degree), including (a) even-span type; (b) modified arch type; (c) Quonset type.

In (2), $Z > 1$ means that the major axis's length is $2Hr$ and the height of the elliptical shape section is longer than its width, which is the case for the Quonset type. If $Z < 1$, the length of the major axis is W, and the width of the elliptical shape section is longer than its height, which is the case for the modified arch type. If $Z = 1$,, then the axis lengths are equal, and the elliptical shape becomes a circular shape.

As shown in Fig. 1b and c, the curved parts are divided into several tilted surfaces. The roof of the modified arch

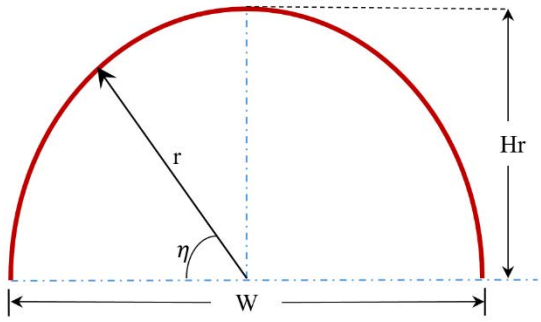

FIGURE 2. A cross section of an elliptic shape in polar coordinates.

greenhouse is divided into six inclined surfaces based on the values of the radius r, so a flat section is considered each 30° ($\eta = 30°, 60°, 90°, 120°, 150°, 180°$). With the same logic, the Quonset greenhouse is subdivided into 12 sections, each 15° degree a section is provided. Therefore, by changing the ellipse aspect ratio, all the possible curved shapes can be analyzed.

B. THE SUN INCIDENCE ANGLE ON AN INCLINED SURFACE

The global solar radiation incident on each surface of the greenhouse is a function of solar angles such as incidence angle (θ), solar declination angle (δ), solar hour angle (ω), surface azimuth angle (γ), latitude of the location (ϕ), and surface inclination angle (β). The most important relation between solar angles related to this study belongs to incidence angle which is the angle between the sun's ray and the considered surface and presented as:

$$\begin{aligned}\cos\theta = {} & \sin\delta\sin\phi\cos\beta - \sin\delta\cos\phi\sin\beta\cos\gamma \\ & + \cos\delta\cos\phi\cos\beta\cos\omega \\ & + \cos\delta\sin\phi\sin\beta\cos\gamma\cos\omega \\ & + \cos\delta\sin\beta\sin\gamma\sin\omega \end{aligned} \tag{3}$$

As it mentioned before, latitude of Rasht city is 37°28′. More details regarding the relations among the solar angles can be found in [39]–[41]. For calculating the hour angle and the time that the sun is in the sky the length of day (DL) is determined by the following equation:

$$\mathrm{DL} = \frac{2}{15}\cos^{-1}(-\tan\phi\tan\delta) \tag{4}$$

Thus, sunrise and sunset for any day can be calculated. The sunrise hour is evaluated by (5) and the sunset hour is the sum of the sunrise and the day length.

$$\text{sunrise} = 12 - \frac{\mathrm{DL}}{2} \tag{5}$$

In calculating the incidence angle (3), surface azimuth angle (γ) is the angle between the south line and the projection of normal vector on horizontal plane of the considered surface. If the angle is in the west side of the south line it is negative and if the angle is on the east side of the south

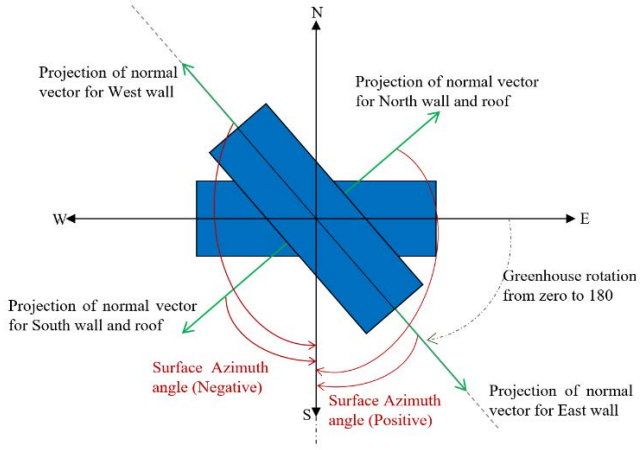

FIGURE 3. Surface azimuth angle for various sections of a greenhouse.

line is positive. Surface azimuth angle is a representative of the greenhouse orientation. This means that for any rotation of the greenhouse from zero degree (E-W) to 180°, surface azimuth angle for each surface should be calculated. The method of obtaining the surface azimuth angle for any orientation of the greenhouse is shown in Figure 3 [41].

C. GLOBAL SOLAR RADIATION ON AN INCLINED SURFACE

In general, The hourly solar irradiance incident on an inclined surface (I_T) consists of three components, namely: the beam radiation I_b, the diffuse radiation I_d, and the reflected radiation from the surrounding environment [39]:

$$I_T = R_b I_b + R_d I_d + \rho_a R_g I \tag{6}$$

In (6) R_b and R_d are the fractions of beam (geometric factor) and diffuse irradiations on a horizontal plane intercepted by the inclined surface, and R_g is the fraction of the reflected radiation from the ground received by that surface. ρ_a is the reflectance of the ground (ground albedo), and assumed 0.2 for soil [42].

First step in determining the hourly solar radiation on a sloped surface is to calculate the hourly diffuse and beam radiation components. These terms are derived from the hourly global solar irradiance I measured by IRIMO in a weather station located in Agricultural Organization of Rasht (37.2° N, 49.5° E) Iran [38]. For this aim, the hourly clearness index k_T defined as:

$$K_T = \frac{I}{I_0} \tag{7}$$

where I_0 is the hourly extraterrestrial irradiation on a horizontal plane between two hour angles ω_1 and $\omega_2(\omega_2 > \omega_1)$:

$$I_0 = \frac{12 \times 3600}{\pi} G_{sc} \left(1 + 0.033 \cos \frac{360n}{365}\right) \times \left[\cos\phi \cos\delta \left(\sin\omega_2 - \sin\omega_1\right) + \frac{\pi\left(\omega_2 - \omega_1\right)}{180} \sin\phi \sin\delta\right] \tag{8}$$

where G_{sc} is extraterrestrial solar irradiance taken $1367 W/m^2$.

Then, the Erbs *et al.* [41], [43] correlation as a function of the hourly clearness index is used for evaluating the diffuse radiation term I_d as follow:

$$\frac{I_d}{I} = \begin{cases} 1.0 - 0.09 k_T & \text{for } k_T \le 0.22 \\ 0.9511 - 0.1604\, k_T + 4.388\, k_T^2 & \\ \quad -16.638 k_T^3 + 12.336 k_T^4 & \text{for } 0.22 < k_T \le 0.8 \\ 0.165 & \text{for } k_T > 0.8 \end{cases} \tag{9}$$

The Erbs correlation was developed for locations with latitude between 31° and 42°, thus, this correlation can be used for determining the diffuse radiation term in Rasht city in Iran with the latitude of 37°.

By calculating the diffuse radiation term, the direct beam radiation term can be computed as follow:

$$I_b = I - I_d \tag{10}$$

The next step in calculating I_T is to evaluate R_b, R_d, and R_g. The geometric factor (tilt factor) R_b between two hour angles ω_1 and ω_2 ($\omega_2 > \omega_1$) is formulated as [41]:

$$R_b = \frac{a}{b} \tag{11}$$

$$\begin{aligned} a = {} & (\sin\delta \sin\phi \cos\beta - \sin\delta \cos\phi \sin\beta \cos\gamma) \\ & \times (\omega_2 - \omega_1) \frac{\pi}{180} \\ & + (\cos\delta \cos\phi \cos\beta + \cos\delta \sin\phi \sin\beta \cos\gamma) \\ & \times (\sin\omega_2 - \sin\omega_1) \\ & - (\cos\delta \sin\beta \sin\gamma) \times (\sin\omega_2 - \sin\omega_1) \end{aligned} \tag{12}$$

$$\begin{aligned} b = {} & (\cos\delta \cos\phi) \times (\sin\omega_2 - \sin\omega_1) \\ & + (\sin\delta \sin\phi) \times (\omega_2 - \omega_1) \frac{\pi}{180} \end{aligned} \tag{13}$$

In order to calculate the diffuse radiation term on a sloped surface, an anisotropic model called HDKR presented by Reindl *et al.* [41], [44] is used in this research. The anisotropic behavior of the sky is taking into account in this model, which means, beside the isotropic diffuse component, the circumsolar radiation and horizon-brightening terms are also considered in the calculations. According to the HDKR model the fraction of diffuse radiation component (R_d) is defined as [41]:

$$R_d = \left(1 - \frac{I_b}{I_0}\right) \left(\frac{1 + \cos\beta}{2}\right) \left[1 + \sqrt{\frac{I_b}{I}} \sin^3\left(\frac{\beta}{2}\right)\right] + \frac{I_b}{I_0} R_b \tag{14}$$

Lastly, the fraction of reflected solar radiation from the ground intercepted by the sloped surface R_g, in the absence of any barriers, is given by [41], [43]:

$$R_g = \frac{1 - \cos\beta}{2} \tag{15}$$

The aforementioned equations are used to ascertain the global hourly solar radiation falling on each section of the greenhouses. Therefore, the total solar radiation intercepted

by the greenhouse cover is the sum of the hourly solar radiation received by each section and can be written as follow:

$$S_c = \sum_{i=1}^{6} A_i I_{T_i} \tag{16}$$

where A_i and I_{T_i} are the area and hourly solar radiation for ith section of the greenhouse, respectively.

D. CALCULATING GREENHOUSE COVER TRANSMITTANCE FOR SOLAR RADIATION COMPONENTS

The global solar radiation that reaches each surface of the greenhouse is comprised of three parts, as it discussed before, direct beam, diffuse, and reflected. In general, Transmissivity of the cover for each section of a greenhouse for these three components are different, and highly depends on the optical properties of the canopy cover material. These optical properties includes angle of refraction (θ_{rf}), the extinction coefficient (K), and the cover thickness (L). For a greenhouse covered with polyethylene sheets (K $= 400\text{m}^{-1}$ [45] and L $= 200\text{m}^{-1}$), transmittance is determined by the Fresnel and Bouguer's law of attenuation [41]:

$$\tau = e^{-KL/\cos\theta_{rf}} \times \frac{1}{2}\left[\frac{1-r_{\parallel}}{1+r_{\parallel}} + \frac{1-r_{\perp}}{1+r_{\perp}}\right] \tag{17}$$

where $r_{\parallel}$ and $r_{\perp}$ denote the parallel and perpendicular polarization components of the incident solar radiation defined by [41]:

$$r_{\perp} = \frac{\sin^2(\theta_{rf}-\theta_i)}{\sin^2(\theta_{rf}+\theta_i)} \tag{18}$$

$$r_{\parallel} = \frac{\tan^2(\theta_{rf}-\theta_i)}{\tan^2(\theta_{rf}+\theta_i)} \tag{19}$$

The refraction angle θ_{rf} is a function of solar incidence angle θ_i and the refractive index of the medium (n_2) and calculated by Snell's Law as follow: ($n_1 = 1$ and $n_2 = 1.49$)

$$n_1 \sin\theta_i = n_2 \sin\theta_{rf} \tag{20}$$

Since θ_i is the angle of incidence for direct beam radiation, it is used for calculating the transmittance for the beam radiation term. In order to compute the transmittance for the diffuse and reflected radiation terms, effective incidence angle for diffuse θ_d and reflected from the ground θ_{gr} as functions of the surface inclination angle (β) are defined by Duffie and Beckman for replacing θ_i in (20) as follow [41]:

$$\theta_d = 59.7 - 0.1388 \times \beta + 0.001497 \times \beta^2 \tag{21}$$

$$\theta_{gr} = 90 - 0.5788 \times \beta + 0.002693 \times \beta^2 \tag{22}$$

E. DISTRIBUTION OF SOLAR RADIATION INSIDE THE GREENHOUSE

In order to obtain the transmitted solar radiation available in the greenhouse, solar radiation distribution inside the greenhouse should be investigated. Out of the total solar radiation intercepted by the greenhouse cover S_c, a part is reflected back to the air ($\rho \times S_c$) and the rest transmits into the greenhouse system. The transmitted part falls into the different components of the greenhouse such as floor and different sections of greenhouse structure. The part reaching the walls and roofs of the greenhouse structure ($S_t \times F_t$), the inner side of the greenhouse cover, is subdivided into two components either reflects back to the greenhouse system or transfer through the cover and lost to the air. Out of the part that falls into the greenhouse ground, assuming there is no plant in the greenhouse, a fraction is absorbed by the soil and lost to the underground, the rest of it gets back to the greenhouse by convection, evaporation, and radiation. The solar radiation parts that reflect back to the greenhouse environment (from the floor and walls) cause greenhouse effect and increase the air temperature. The fraction of solar radiation received by the floor has the main contribution on greenhouse temperature and greenhouse effect, so optimizing this part could help the researcher in lowering the energy consumption rate in greenhouse cultivation. Figure 4 shows a schematic of solar radiation transmission and its distribution in the greenhouse. In Figure 4, F_t is the total solar fraction.

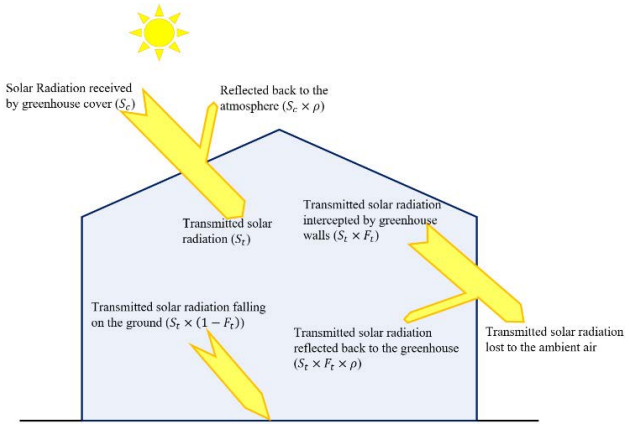

FIGURE 4. Solar radiation distribution inside the greenhouse.

1) TRANSMITTED SOLAR RADIATION AVAILABILITY INSIDE THE GREENHOUSE

Based on the calculated transmittance of various solar radiation components, the hourly solar radiation transmitted inside a greenhouse S_t between hour angles ω_1 and ω_2 can be written as:

$$S_t = \sum\left(\begin{pmatrix} R_b I_b \times \tau_b \times (1-\rho_b) + R_d I_d \times \tau_d \times (1-\rho_d) \\ +\rho_a R_g I_g \times \tau_{gr} \times (1-\rho_{gr}) \end{pmatrix} \times A_i\right) \tag{23}$$

where ρ is the reflectance of the cover for three components of solar radiation and it is calculated assuming that canopy cover cannot absorb radiation so the absorptance of the polyethylene sheet is taking zero. Thus:

$$\rho = 1 - \tau \tag{24}$$

According to the described solar radiation distribution in the greenhouse (Figure 4), transmitted solar radiation available in the greenhouse consists of two parts: the part of

radiation reaching the ground (S_{floor}) and the reflected part of transmitted solar radiation intercepted by the walls and roofs (S_{ref}). The total hourly transmitted solar radiation available in the greenhouse system is formulated as:

$$S = S_{ref} + S_{floor} \tag{25}$$

$$S_{floor} = S_t \times (1 - F_t) \tag{26}$$

$$S_{ref} = S_t \times \rho \times F_t \tag{27}$$

In calculating S_{ref} (27), the solar incidence angle for different components of transmitted solar radiation reaching the inner side of the greenhouse cover cannot be ascertained, thus, the reflectance of the cover (ρ) is taken as 0.1 for the inside part of the cover [46]. The term F_t in (26) and (27) is the total solar fraction and it is explained in the next subsection.

As a result, hourly solar radiation available inside the greenhouse can be obtained for a day from sunrise to sunset. Three MATLAB scripts are written in MATLAB R2018b software for each types of greenhouses to calculate the hourly solar radiation inside the three greenhouse for all the possible dimensions and orientations in Rasht city. Thus, the daily and monthly solar radiation also can be easily determined. It should be noted that because the floor area of the greenhouses is constant, the solar radiation losses to the ground are equal for each floor area; therefore, to optimize the amount of available solar radiation inside the greenhouse, this part of radiation loss could be neglected.

2) TOTAL SOLAR FRACTION

From Figure 4, it can be deduced that solar radiation transmitted into the greenhouse basically is divided in two segments; the part falling on the greenhouse ground ($S_t \times (1 - F_t)$) and the part reaching the greenhouse structure ($S_t \times F_t$) (walls and roofs). The magnitude of the total solar fraction is the key to determining the fractions of these two fractions of transmitted solar radiation inside the greenhouse. The total solar fraction is a representative of radiation loss through the greenhouse sections and it is defined as the ratio of the sum of the solar radiation intercepted by various sections of the greenhouse (walls and roofs) to the total solar radiation transmitted into the greenhouse system. Therefore, total solar fraction is a function of solar angles and the solar radiation components on each surface of the greenhouse [47].

The method used in this study for evaluating the total solar fraction is the three dimensional (3D) shadow analysis, which is a drawing technique presented by Gupta *et al.* [47]. For this purpose, for each greenhouse type and each floor area and based on the range of variation for each decision variable, the total solar fraction for various dimensions at five different orientations (0°, 30°, 45°, 60°, 90°) is calculated. The range of variation for each parameter is subdivided into four equal parts. Therefore, a set of values for each parameter is obtained. Total solar fractions for each greenhouse based on the obtained dimensions are calculated for the considered orientations in winter and summer. The values of F_t for other orientations and sizes in the optimization process were obtained by interpolating the existing values. For an even-span greenhouse and for floor area of 60m^2 as an example, limitation for length is between 8 m and 12 m, for the height of walls is 2 m to 5 m and for roof's height is 0.3 m to 3 m, so all the possible dimensions for constructing an even-span greenhouse equal to 48 states. The total solar fraction for these 48 states for five considered orientations in each week of two considered time periods in winter and summer based on the 3D shadow analysis is computed in Auto CAD 2013 software, and for other dimensions, orientations, and times, F_t is computed by interpolation.

F. OPTIMIZATION MODELING

The main purpose of multi-objective optimization of the three considered greenhouse types is to optimize the design parameters (dimension and orientation) for each greenhouse types for optimal use of solar radiation throughout a year. Optimal use of solar radiation in a greenhouse means maximizing the solar energy inside the greenhouse in winter and minimizing it in summer, which leads to extending the usage of greenhouse cultivation in a year. To this end, the average hourly solar radiation available inside the greenhouse in winter and summer are defined as two objective functions. Two time periods in winter and summer are selected based on the intensity of solar radiation, for winter (first objective function) the time period is from 1st January to 30th February when the solar irradiation intensity is low and for summer (second objective function) the time period is from 1st June to 30th July when the solar intensity is high. These two objective functions are expressed by (25). Therefore, the goal of using multi-objective optimization is to simultaneous maximizing the transmitted solar radiation into the greenhouse in winter for heating purposes and minimizing the transmitted solar radiation in summer for lowering the required energy for cooling.

Decision variables in this study are the physical parameters needed for constructing the considered greenhouses including length, width, height of the different section, and ellipse aspect ratio for the curved shape sections. In addition, for a more realistic comparison and investigating effect of size of the greenhouse on the result of the optimization, three different floor area sizes (30m^2, 60m^2, and 120m^2) are considered and the multi-objective optimization process is conducted for each greenhouse types and each floor area sizes. Decision variables and their range of variations based on the size of the floor area for each types of greenhouse including even-span, modified arch, and Quonset are defined and presented in Tables 1a-c, respectively. The range considered for each decision variable is based on the feasibility of constructing a typical greenhouse [48]. In addition, for the total height of the modified arch and Quonset greenhouses an additional constraint is imposed on the optimization procedure as follows:

$$2 < H_T < 10 \tag{28}$$

$$H_T = H_{wall} + H_{roof} \tag{29}$$

where H_T is the total height of the greenhouse, in modified arch types equal to the sum of the wall and roof heights, and in Quonset type equals the height of roof (curved section).

The multi-objective optimization genetic algorithm (MOGA) is used for optimizing the defined maximization-minimization problem. The population size for each generation is defined based on the number of decision variables, for even-span and modified arch greenhouses with four decision variables the population size is taken as 70 individuals and for Quonset greenhouse with three decision variables, 50 individuals are considered for the population size.

III. RESULT AND DISCUSSION

The optimization is conducted for northern Iran climate conditions and a case study of the city of Rasht. Typical weather data are obtained from the Iran Meteorological Organization. Three common types of single-span greenhouses are optimized; for each type, three-floor areas are considered, and optimization processes are performed for each of them. Therefore, nine optimal answers are obtained. Values of decision variables (design parameters) for each greenhouse are presented in Tables 2a-2c.

Result of multi-objective optimization for the even-span type (Table 1a) and all floor area sizes shows that the best orientation is zero degree or (E-W) direction. In addition, the optimal length of the even-span greenhouse, regardless of its size (floor area), equals the upper band of the considered range of variation. This means that the length of an even-span greenhouse should be taken as the maximum possible amount based on its floor area. In other words, the length to width ratio (L/W) in an even span greenhouse should be maximized to increase the amount of solar energy in winter. The optimum height for walls of an even-span greenhouse for all floor area sizes is approximately 3.8 m, which means that for all even-span greenhouse sizes, the best height for the walls is between 3.7 m and 3.90 m. With regard to the roof height, this design parameter is an indication of the angle between tilt sections and the horizontal line. The results show that the angle of the roof tilt surfaces with the horizontal line remains almost unchanged with increasing greenhouse size. This angle for $30m^2$, $60m^2$, and $120m^2$ of floor area is 15.2°, 16.2°, and 16° for the efficient use of greenhouses in cold and hot seasons in the location of this study.

For the modified arch greenhouse, similar to the even-span greenhouse, the optimal direction is E-W, and the optimal length is equal to the maximum possible length according to the ground area size (Table 1b). The heights of walls for small and large modified arch greenhouses ($30m^2$ and $120m^2$) are the same, but for medium-sized greenhouses, the height of walls is one meter higher. On the other hand, the height of the roof based on the ellipse aspect ratio (2) ($Z = 0.25$) for $60m^2$ floor area is 0.65 m and for small and large floor area sizes equal to 1.5 m and 2 m, respectively, which means that for a modified arch greenhouse, the size of the floor area plays an important role in selecting the optimal height for walls and curved roofs. The height of the walls and the ellipse aspect ratio are two components of the total height of the greenhouse, and based on the result of optimization, the total heights for $30m^2$, $60m^2$, and $120m^2$ of the floor area are 4.55 m, 4.72 m, and 5.12 m, respectively. The total height of the modified arch greenhouse increases with the floor area sizes. This is because the value of the total solar fraction decreases with increasing greenhouse length.

The optimal answers of multi-objective optimization for the Quonset type (Table 1c) shows that the orientation and length of the greenhouse are similar to those of the other two shapes, E-W orientation and maximum length. The total height of the greenhouse or the height of the curved section for this case indicates that the greenhouse with the largest floor area has the greatest height among all three considered greenhouse sizes. The total heights for the $30m^2$, $60m^2$, and $120m^2$ floor areas are calculated from the ellipse aspect ratio and are equal to 6.5 m, 7.5 m, and 8 m, respectively. The height of the greenhouse increases with the size of the floor area for the Quonset type. Therefore, in a single span Quonset greenhouse, a relation can be defined between the width of the greenhouse and ellipse aspect ratio. $\frac{Z}{W}$ The ratios for $60m^2$ and $120m^2$ are equal to 0.62 and 0.64, respectively, and for small greenhouses, the ratio is 0.8. This means that for medium- and large-sized greenhouses, this ratio should be 0.6, and for small greenhouses, it should be equal to 0.8. Therefore, by introducing $\frac{Z}{W}$ the concept for Quonset greenhouses, greenhouse owners are capable of optimum use of solar energy and increase the usage of greenhouses beyond the traditional use of greenhouses in a year. Moreover, the total height of the Quonset greenhouse is also higher than even-span and modified arch greenhouses by a considerable margin for all the floor area sizes. This could be explained by the lack of vertical surfaces for this type. Additionally, it can be noted that by increasing the height, the northern section receives a smaller amount of solar radiation in summers.

Values of objective functions for each greenhouse type and three different floor areas are shown in Figs. 5a-c. Comparing the amount of solar radiation available inside a greenhouse on winter days and summer days, it can be seen that solar radiation inside the even-span and modified arch greenhouses for $60m^2$, and $120m^2$ in summer days is twice as high as that in winter days, and for $30m^2$, the floor area equals 1.7. This ratio for Quonset type is much lower for all floor area sizes of 1.22, 1.4, and 1.22 for $30m^2$, $60m^2$, and $120m^2$, respectively. As shown in Fig. 5c, the Quonset type has the best performance in capturing the maximum solar energy in winter days and the minimum amount of solar radiation in summer days for all three greenhouse sizes compared to the two other types.

It should be noted that although Quonset-type greenhouses have the highest amount of captured solar energy in winter and the lowest in summer, the total height of Quonset greenhouses is higher than that of the two other types for all floor area sizes. On the other hand, the difference in total height between even-span and modified arch types for three considered floor areas are 30 cm, 20 cm, and 50 cm from

TABLE 1. (a) Decision variables and their range of variation for the even-span greenhouse. (b) Decision variables and their range of variation for the modified arch greenhouse. (c) Decision variables and their range of variation for the Quonset greenhouse.

(a)

	Range of variation based on the floor area (A_f)		
Decision variables	$A_f = 30\text{m}^2$	$A_f = 60\text{m}^2$	$A_f = 120\text{m}^2$
Length of the greenhouse (m)	$6 \le L \le 9$	$8 \le L \le 12$	$12 \le L \le 24$
Height of the walls (m)	$2 \le H_{wall} \le 5$	$2 \le H_{wall} \le 5$	$2 \le H_{wall} \le 5$
Height of the roof (m)	$0.2 \le H_{roof} \le 3$	$0.2 \le H_{roof} \le 3$	$0.2 \le H_{roof} \le 3$
Angle of greenhouse rotation (rad)	$0 \le \Theta_{rotat} \le \pi$	$0 \le \Theta_{rotat} \le \pi$	$0 \le \Theta_{rotat} \le \pi$

(b)

	Range of variation based on the floor area (A_f)		
Decision variables	$A_f = 30\text{m}^2$	$A_f = 60\text{m}^2$	$A_f = 120\text{m}^2$
Length of the greenhouse (m)	$6 \le L \le 9$	$8 \le L \le 12$	$12 \le L \le 24$
Height of the walls (m)	$2 \le H_{wall} \le 5$	$2 \le H_{wall} \le 5$	$2 \le H_{wall} \le 5$
Ellipse aspect ratio of the roof	$0 \le Z \le 1$	$0 \le Z \le 1$	$0 \le Z \le 1$
Angle of greenhouse rotation (rad)	$0 \le \Theta_{rotat} \le \pi$	$0 \le \Theta_{rotat} \le \pi$	$0 \le \Theta_{rotat} \le \pi$

(c)

	Range of variation based on the floor area (A_f)		
Decision variables	$A_f = 30\text{m}^2$	$A_f = 60\text{m}^2$	$A_f = 120\text{m}^2$
Length of the greenhouse (m)	$6 \le L \le 9$	$8 \le L \le 12$	$12 \le L \le 24$
Ellipse aspect ratio	$0 \le Z \le 4$	$0 \le Z \le 4$	$0 \le Z \le 4$
Angle of greenhouse rotation (rad)	$0 \le \Theta_{rotat} \le \pi$	$0 \le \Theta_{rotat} \le \pi$	$0 \le \Theta_{rotat} \le \pi$

small to large size, which are negligible in constructing a greenhouse.

To provide a better insight into the effect of shape and size on the amount of transmitted solar energy inside the greenhouse, the total solar fraction for each greenhouse types in two clear days in winter (January) and summer (June) is shown in Figs. 6a-c. Since the solar fraction is directly related to the physical parameters of the greenhouse and the sun irradiance, it is an ideal parameter for investigating the radiation received by the greenhouse ground and the radiation loss through the cover. The total solar fraction (F_t) decreases by increasing the floor area sizes (increasing the length) in each hour of the day and for all greenhouse types.

For even-span and modified arch types from Fig. 6a and b, it can be realized that on summer day and during times when sun insolation is intense (9:00 AM to 17:00 PM), the total solar fraction for all floor area sizes is between 0.25 and 0.15, which means that a great part of solar radiation falls into the greenhouse ground. The total solar fraction for the large greenhouse (120m^2) in the mentioned period of time is approximately 0.15 for even-span and modified arch greenhouses.

With regard to the Quonset type, it can be seen from Fig. 6c that the value of the total solar fraction for a summer day at noon is approximately 0.3, which is much higher than the other two types, and for winter days, F_t throughout the day does not have a wide range of variation for all floor area sizes. The values of the total solar fraction for Quonset type are the main reason for its better performance in capturing solar energy in comparison to even-span and modified arch types.

The most frequently cultivated crops in the greenhouse industry are mainly vegetables, which need medium thermal requirements. The FAO set the minimum daily solar radiation limit of 8.5 $\text{MJ m}^{-2}\ \text{day}^{-1}$ (2.34 $\text{kWh m}^{-2}\ \text{day}^{-1}$) for summer crops [49], below which these crops cannot grow. Therefore, an optimized greenhouse should be able to satisfy

TABLE 2. (a) Values of design parameters for the even-span type based on floor area size. (b) Values of design parameters for the modified arch type based on floor area size. (c) Values of design parameters for the Quonset type based on floor area size.

(a)

Decision Variables	$A_f = 30\text{m}^2$	$A_f = 60\text{m}^2$	$A_f = 120\text{m}^2$
L (m)	8.90	11.95	23.90
H_{wall} (m)	3.8	3.75	3.9
H_{roof} (m)	0.44	0.73	0.72
Θ_{rotat} (rad)	0.0	0.0	0.0

(b)

Decision Variables	$A_f = 30\text{m}^2$	$A_f = 60\text{m}^2$	$A_f = 120\text{m}^2$
L (m)	8.98	11.92	23.97
H_{wall} (m)	3.14	4.1	3.12
Z	0.85	0.25	0.8
Θ_{rotat} (rad)	0.0	0.0	0.0

(c)

Decision Variables	$A_f = 30\text{m}^2$	$A_f = 60\text{m}^2$	$A_f = 120\text{m}^2$
L (m)	8.5	11.85	23.93
Z	3.7	3.1	3.2
Θ_{rotat} (rad)	0.0	0.0	0.0

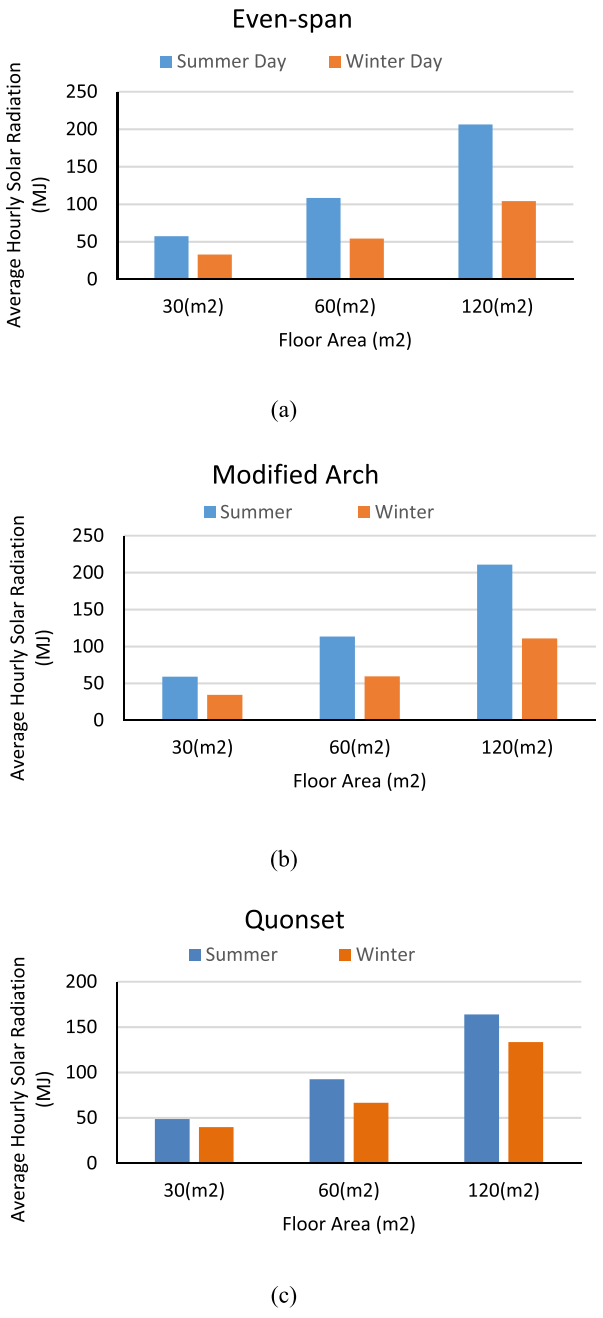

FIGURE 5. Values of objective functions for each floor area size and greenhouse type: (a) even-span type; (b) modified arch; (c) Quonset.

the minimum criteria for solar radiation for the maximum possible days yearly, particularly in cold seasons.

Based on the obtained decision variables from the multi-objective optimization procedure, the daily solar radiation available inside the greenhouse per square meter during an entire year for each greenhouse type and three-floor area sizes are shown in Figs. 7a-c. These figures show the minimum solar radiation limitation proposed by FAO with a red dotted line. For all types of greenhouses, the daily solar radiation per square meter inside the greenhouse, for a specific time, decreases with increasing greenhouse ground size.

From Fig. 7, it can be seen that the greenhouse built with the optimized design parameters can provide an environment in which offseason vegetables can grow in most of the months in a year in the location of this investigation.

The values of solar radiation per square meter for the modified arch greenhouse are larger than the even-span type for each floor area size. However, the difference between their values is small. The yearly performance of even-span and modified arch types Fig. 7b and 7c shows that the optimized parameters can satisfy the need for solar radiation in most months of the year except two cold months (January and December) in winter for medium and large size even-span greenhouse, and one month (December) for medium size and two months (January and December) for large size modified arch type.

Despite its greater height, the yearly performance of Quonset type is better than two other shapes by a considerable margin, especially in summers when the solar radiation

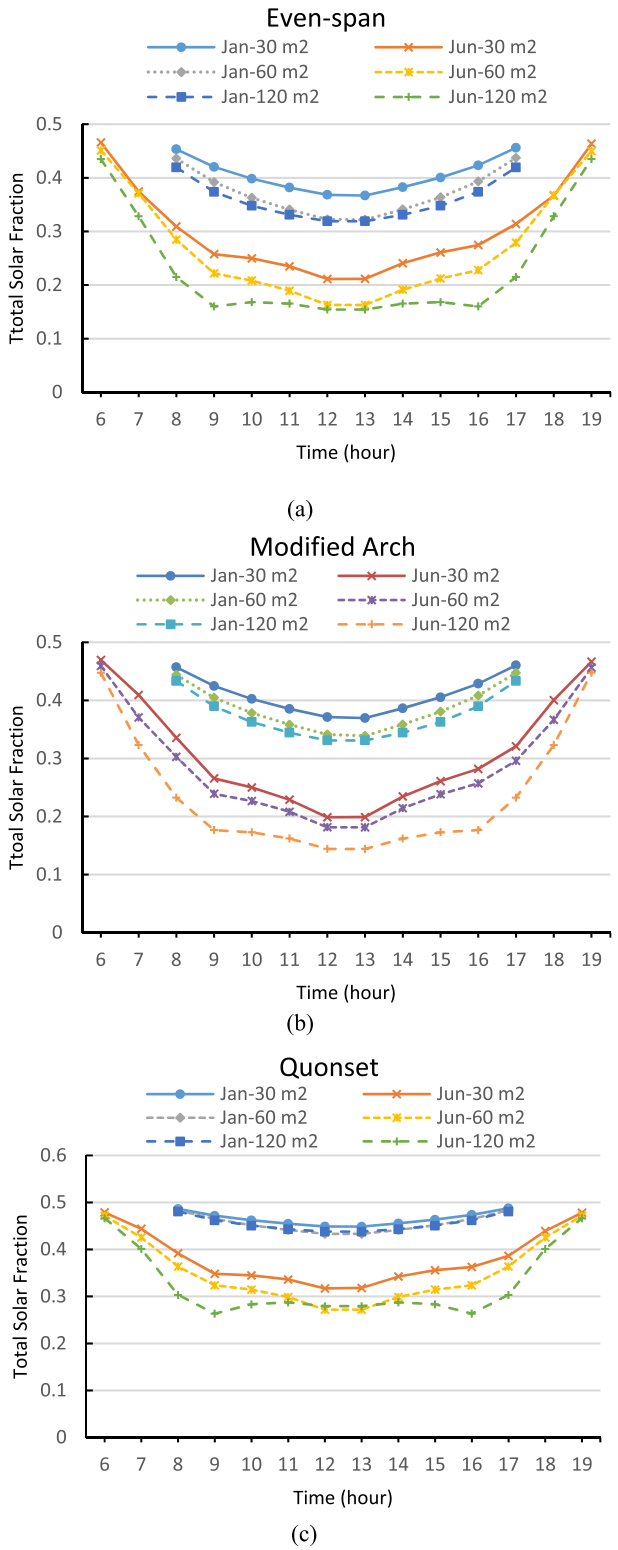

FIGURE 6. The total solar fraction at different floor area sizes on summer days and winter days: (a) even span; (b) modified arch; (c) Quonset.

works against the energy usage for cooling and ventilation. As shown in Fig. 7c, the Quonset-type greenhouse has superior performance in cold seasons compared to the other types,

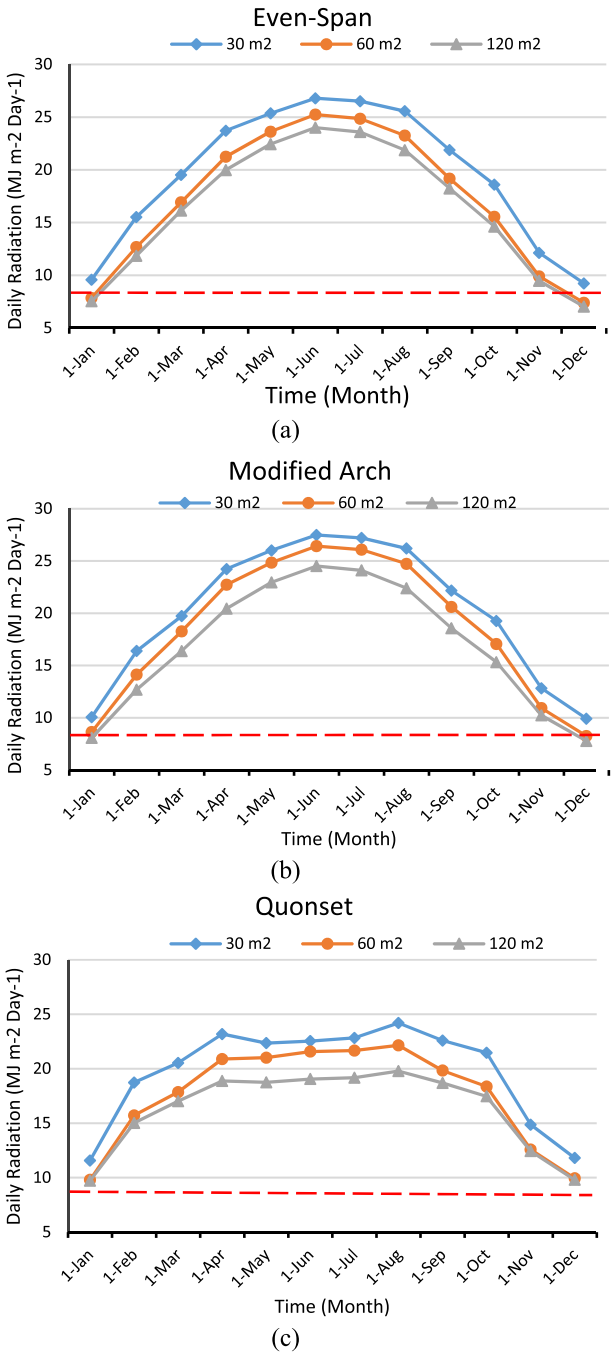

FIGURE 7. Yearly performance of available solar radiation per square meter inside the greenhouse: (a) even span; (b) modified arch; (c) Quonset.

especially in November, December, January, and February, when the need for solar energy is higher. On the other hand, in months such as May, June, July, and August, the amount of solar radiation inside the greenhouse for Quonset type is lower than both modified arch and even-span types, which could be an advantage because solar energy is abundant. There is a need for cooling and ventilation in greenhouse cultivation, especially in areas with hot summers, such as northern Iran.

TABLE 3. Values of design parameters for the Quonset type based on floor area size.

No	Name	Solar Radiation Model	Aim of the study	Location & Climate	Limitation of the Study
1	Present Study	anisotropic	Efficient use of solar radiation	Rasht Iran, Subtropical climate	-
2	El-Maghlany 2015[17]		Maximize the solar radiation received by the floor	Latitudes 21° to 24° and Cold Climate	Radiation loss
3	Çakir 2015[18]	Isotropic	Maximize the Solar radiation in winter	Bayburt Turkey, Cold Climate	Total Height and Solar Radiation on the cover is considered
4	Chen 2020[16]	Isotropic	Maximize the Solar radiation in winter	Southern Areas of China, Subtropical Climate	Radiation loss and Greenhouse dimensions

A comparison between this study and similar studies about modeling the solar radiation in a greenhouse is presented in Table 3. Solar model, goal of the study as well as the location and climate condition of each studies are compared and the limitation of each study is also presented. As it can be seen from Table 3, the model used for investigating the solar radiation in previous studies is isotropic model, but estimation of solar radiation is improved in this study by considering an anisotropic model. However, the most significant difference between this work and previous ones is in the goal of this research and employing a multi-objective optimization technique for obtaining the optimal greenhouse design parameters in order to use the solar radiation efficiently throughout a year instead of just focusing on maximizing the solar radiation in cold months. This approach could help the greenhouse owners to extend the usage of greenhouse cultivation beyond the traditional use of a greenhouse.

IV. CONCLUSION

The amount of solar radiation available inside a greenhouse mainly depends on its shape, structure and orientation. Therefore, the current study presents an optimization methodology for the efficient use of solar energy based on the key physical parameters of different greenhouses. The main goal is to extend the growing calendars beyond the conventional greenhouse cultivation season in the northern areas of Iran, specifically the case study of Rasht city. The proposed method also suggested a novel technique to include the total solar fraction for estimating solar radiation loss from various sections of a greenhouse and to calculate the available solar energy inside the greenhouse. It was found that integrating the suggested mathematical model with the multi-objective optimization (MOGA) method for the simultaneous optimization of two conflicting objective functions leads to the development of a set of physical parameters for the greenhouse that results in maximizing the usage of solar energy in winter and minimizing that in summer. The following conclusions can be drawn mainly based on the results of multi-objective optimization:

- For three investigated greenhouses (even-span, modified arch, Quonset), the best direction of placement is E-W orientation, and the optimal length is the maximum possible length or length to width ratio that should be maximized.
- In an even-span greenhouse, regardless of its size, the optimal wall height and roof inclination angle are approximately 3.7 m and 16°, respectively. Furthermore, small even-span greenhouses are more efficient than medium and large greenhouses according to the values of the total solar fraction and available solar radiation per square meter in the greenhouse.
- For the modified arch type, the values of the decision variables for small and large floor area sizes are close to each other (Hw $=$ 3.1 m and Z $=$ 0.8). The medium-sized modified arch greenhouse has the highest wall height and lowest ellipse aspect ratio. The modified arch greenhouse with 60m^2 has better performance in using solar radiation than two other sizes.
- In a Quonset greenhouse, the optimal $\frac{Z}{W}$ ratio, introduced for the first time in this study, for 60m^2 and 120m^2 floor area sizes is 0.6, and for small size, greenhouse is 0.8. This ratio will help farmers find the optimal physical parameters based on the ground area sizes to build a Quonset greenhouse. A large size Quonset greenhouse is more efficient than small and medium sizes. Moreover, the Quonset greenhouse has the best performance in capturing solar radiation per square meter and values of total solar fraction than even-span and modified arch types in northern areas of Iran.

The result of the multi-objective optimization can be used for the northern area in Iran and the similar latitude in other countries. Moreover, the presented optimization method in this study can be extended for other locations in northern

hemisphere and climates to select the suitable orientation and dimensions of different greenhouses for the most efficient usage of solar energy.

REFERENCES

[1] *The Future of Food and Agriculture: Trends and Challenges*. Rome, Italy: Food and Agriculture Organization of the United Nations, 2018.

[2] A. Vadiee and V. Martin, "Energy management in horticultural applications through the closed greenhouse concept, state of the art," *Renew. Sustain. Energy Rev.*, vol. 16, no. 7, pp. 5087–5100, Sep. 2012, doi: 10.1016/j.rser.2012.04.022.

[3] M. Esen and T. Yuksel, "Experimental evaluation of using various renewable energy sources for heating a greenhouse," *Energy Buildings*, vol. 65, pp. 340–351, Oct. 2013, doi: 10.1016/j.enbuild.2013.06.018.

[4] L. Schiller, *The Year-round Solar Greenhouse: How to Design and Build a Net-Zero Energy Greenhouse*. Gabriola, BC, Canada: New Society Publishers, 2016.

[5] J. G. Pieters and J. M. Deltour, "Modelling solar energy input in greenhouses," *Sol. Energy*, vol. 67, nos. 1–3, pp. 119–130, Jul. 1999, doi: 10.1016/S0038-092X(00)00054-2.

[6] X. Fei, W. Xiao-Long, and X. Yong, "Development of energy saving and rapid temperature control technology for intelligent greenhouses," *IEEE Access*, vol. 9, pp. 29677–29685, 2021, doi: 10.1109/ACCESS.2021.3059199.

[7] A. F. Subahi and K. E. Bouazza, "An intelligent IoT-based system design for controlling and monitoring greenhouse temperature," *IEEE Access*, vol. 8, pp. 125488–125500, 2020, doi: 10.1109/ACCESS.2020.3007955.

[8] F. S. Javadi, H. S. C. Metselaar, and P. Ganesan, "Performance improvement of solar thermal systems integrated with phase change materials (PCM), a review," *Sol. Energy*, vol. 206, pp. 330–352, Aug. 2020, doi: 10.1016/j.solener.2020.05.106.

[9] S. Mahdavi, F. Sarhaddi, and M. Hedayatizadeh, "Energy/exergy based-evaluation of heating/cooling potential of PV/T and Earth-air heat exchanger integration into a solar greenhouse," *Appl. Thermal Eng.*, vol. 149, pp. 996–1007, Feb. 2019, doi: 10.1016/j.applthermaleng.2018.12.109.

[10] A. Chaysaz, S. R. M. Seyedi, and A. Motevali, "Effects of different greenhouse coverings on energy parameters of a photovoltaic–thermal solar system," *Sol. Energy*, vol. 194, pp. 519–529, Dec. 2019, doi: 10.1016/j.solener.2019.11.003.

[11] D. Piscia, J. I. Montero, B. Bailey, P. Muñoz, and A. Oliva, "A new optimisation methodology used to study the effect of cover properties on nighttime greenhouse climate," *Biosyst. Eng.*, vol. 116, no. 2, pp. 130–143, Oct. 2013, doi: 10.1016/j.biosystemseng.2013.07.005.

[12] D. Mazzeo, C. Baglivo, S. Panico, and P. M. Congedo, "Solar greenhouses: Climates, glass selection, and plant well-being," *Sol. Energy*, vol. 230, pp. 222–241, Dec. 2021, doi: 10.1016/j.solener.2021.10.031.

[13] H. Ghasemi Mobtaker, Y. Ajabshirchi, S. F. Ranjbar, and M. Matloobi, "Solar energy conservation in greenhouse: Thermal analysis and experimental validation," *Renew. Energy*, vol. 96, pp. 509–519, Oct. 2016, doi: 10.1016/j.renene.2016.04.079.

[14] H. G. Mobtaker, Y. Ajabshirchi, S. F. Ranjbar, and M. Matloobi, "Simulation of thermal performance of solar greenhouse in north-west of Iran: An experimental validation," *Renew. Energy*, vol. 135, pp. 88–97, May 2019, doi: 10.1016/j.renene.2018.10.003.

[15] M. Taki, Y. Ajabshirchi, S. F. Ranjbar, A. Rohani, and M. Matloobi, "Modeling and experimental validation of heat transfer and energy consumption in an innovative greenhouse structure," *Inf. Process. Agricult.*, vol. 3, no. 3, pp. 157–174, Sep. 2016, doi: 10.1016/j.inpa.2016.06.002.

[16] J. Chen, Y. Ma, and Z. Pang, "A mathematical model of global solar radiation to select the optimal shape and orientation of the greenhouses in southern China," *Sol. Energy*, vol. 205, pp. 380–389, Jul. 2020, doi: 10.1016/j.solener.2020.05.055.

[17] W. M. El-Maghlany, M. A. Teamah, and H. Tanaka, "Optimum design and orientation of the greenhouses for maximum capture of solar energy in north tropical region," *Energy Convers. Manage.*, vol. 105, pp. 1096–1104, Nov. 2015, doi: 10.1016/j.enconman.2015.08.066.

[18] U. Çakir and E. Şahin, "Using solar greenhouses in cold climates and evaluating optimum type according to sizing, position and location: A case study," *Comput. Electron. Agricult.*, vol. 117, pp. 245–257, Sep. 2015, doi: 10.1016/j.compag.2015.08.005.

[19] N. Choab, A. Allouhi, A. E. Maakoul, T. Kousksou, S. Saadeddine, and A. Jamil, "Effect of greenhouse design parameters on the heating and cooling requirement of greenhouses in Moroccan climatic conditions," *IEEE Access*, vol. 9, pp. 2986–3003, 2021, doi: 10.1109/ACCESS.2020.3047851.

[20] N. Choab, A. Allouhi, A. El Maakoul, T. Kousksou, S. Saadeddine, and A. Jamil, "Review on greenhouse microclimate and application: Design parameters, thermal modeling and simulation, climate controlling technologies," *Sol. Energy*, vol. 191, pp. 109–137, Oct. 2019, doi: 10.1016/j.solener.2019.08.042.

[21] B. Mohammadi, S. F. Ranjbar, and Y. Ajabshirchi, "Application of dynamic model to predict some inside environment variables in a semi-solar greenhouse," *Inf. Process. Agricult.*, vol. 5, no. 2, pp. 279–288, Jun. 2018, doi: 10.1016/j.inpa.2018.01.001.

[22] J. Chen, J. Zhao, F. Xu, H. Hu, Q. Ai, and J. Yang, "Modeling of energy demand in the greenhouse using PSO-GA hybrid algorithms," *Math. Problems Eng.*, vol. 2015, Feb. 2015, Art. no. 871075, doi: 10.1155/2015/871075.

[23] A. Mellalou, W. Riad, A. Mouaky, A. Bacaoui, and A. Outzourhit, "Optimum design and orientation of a greenhouse for seasonal winter drying in Morocco under constant volume constraint," *Sol. Energy*, vol. 230, pp. 321–332, Dec. 2021, doi: 10.1016/j.solener.2021.10.050.

[24] B. Mahjoob Karambasti, M. Ghodrat, M. Naghashzadegan, and G. Ghorbani, "Multi-objective optimisation of available solar energy inside a greenhouse in northern Iran," *Int. J. Ambient Energy*, p. 12, May 2022, doi: 10.1080/01430750.2022.2063180.

[25] A. Karami, G. H. Roshani, E. Nazemi, and S. Roshani, "Enhancing the performance of a dual-energy gamma ray based three-phase flow meter with the help of grey wolf optimization algorithm," *Flow Meas. Instrum.*, vol. 64, pp. 164–172, Dec. 2018.

[26] S. Roshani and S. Roshani, "A compact coupler design using meandered line compact microstrip resonant cell (MLCMRC) and bended lines," *Wireless Netw.*, vol. 27, no. 1, pp. 677–684, Jan. 2021.

[27] S. K. Bavandpour, S. Roshani, A. Pirasteh, S. Roshani, and H. Seyedi, "A compact lowpass-dual bandpass diplexer with high output ports isolation," *AEU-Int. J. Electron. Commun.*, vol. 135, Jun. 2021, Art. no. 153748.

[28] F. Parandin and N. Mahtabi, "Design of an ultra-compact and high-contrast ratio all-optical NOR gate," *Opt. Quantum Electron.*, vol. 53, no. 12, pp. 1–9, Dec. 2021.

[29] A. Vahdati and F. Parandin, "Antenna patch design using a photonic crystal substrate at a frequency of 1.6 THz," *Wireless Pers. Commun.*, vol. 109, no. 4, pp. 2213–2219, Dec. 2019.

[30] M. Abdollahi and F. Parandin, "A novel structure for realization of an all-optical, one-bit half-adder based on 2D photonic crystals," *J. Comput. Electron.*, vol. 18, no. 4, pp. 1416–1422, Dec. 2019.

[31] P. Lalbakhsh, B. Zaeri, A. Lalbakhsh, and M. N. Fesharaki, "AntNet with reward-penalty reinforcement learning," in *Proc. 2nd Int. Conf. Comput. Intell., Commun. Syst. Netw.*, Jul. 2010, pp. 17–21.

[32] M. Hookari, S. Roshani, and S. Roshani, "Design of a low pass filter using rhombus-shaped resonators with an analyticalLC equivalent circuit," *Turkish J. Elect. Eng. Comput. Sci.*, vol. 28, no. 2, pp. 865–874, 2020.

[33] A. Pirasteh, S. Roshani, and S. Roshani, "A modified class-F power amplifier with miniaturized harmonic control circuit," *AEU-Int. J. Electron. Commun.*, vol. 97, pp. 202–209, Dec. 2018.

[34] B. Mahjoob Karambasti, M. Ghodrat, G. Ghorbani, A. Lalbakhsh, and M. Behnia, "Design methodology and multi-objective optimization of small-scale power-water production based on integration of stirling engine and multi-effect evaporation desalination system," *Desalination*, vol. 526, Mar. 2022, Art. no. 115542.

[35] H. Saghaei, A. Zahedi, R. Karimzadeh, and F. Parandin, "Line defects on As_2Se_3-chalcogenide photonic crystals for the design of all-optical power splitters and digital logic gates," *Superlattices Microstructures*, vol. 110, pp. 133–138, Oct. 2017.

[36] M. M. Karkhanehchi, F. Parandin, and A. Zahedi, "Design of an all optical half-adder based on 2D photonic crystals," *Photonic Netw. Commun.*, vol. 33, no. 2, pp. 159–165, Apr. 2017.

[37] F. Parandin, M.-R. Malmir, and M. Naseri, "All-optical half-subtractor with low-time delay based on two-dimensional photonic crystals," *Superlattices Microstruct.*, vol. 109, pp. 437–441, Sep. 2017.

[38] (2019). *Iran Meteorological Organization*. Accessed: Dec. 20, 2019. [Online]. Available: http://www.irimo.ir/

[39] S. Mousavi Maleki, H. Hizam, and C. Gomes, "Estimation of hourly, daily and monthly global solar radiation on inclined surfaces: Models revisited," *Energies*, vol. 10, no. 1, p. 134, Jan. 2017.
[40] F. C. McQuiston and J. D. Parker, *Heating, Ventilating, and Air Conditioning: Analysis and Design*. Hoboken, NJ, USA: Wiley, 1988.
[41] J. A. Duffie and W. A. Beckman, *Solar Engineering of Thermal Processes*. Hoboken, NJ, USA: Wiley, 2013.
[42] C. A. Gueymard, "Direct and indirect uncertainties in the prediction of tilted irradiance for solar engineering applications," *Sol. Energy*, vol. 83, no. 3, pp. 432–444, Mar. 2009, doi: 10.1016/j.solener.2008.11.004.
[43] D. G. Erbs, S. A. Klein, and J. A. Duffie, "Estimation of the diffuse radiation fraction for hourly, daily and monthly-average global radiation," *Sol. Energy*, vol. 28, no. 4, pp. 293–302, 1982, doi: 10.1016/0038-092X(82)90302-4.
[44] D. T. Reindl, W. A. Beckman, and J. A. Duffie, "Evaluation of hourly tilted surface radiation models," *Sol. Energy*, vol. 45, no. 1, pp. 9–17, Jan. 1990, doi: 10.1016/0038-092X(90)90061-G.
[45] L. C. Godbey, T. E. Bond, and H. F. Zornig, "Transmission of solar and long-wavelength energy by materials used as covers for solar collectors and greenhouses," *Trans. ASAE*, vol. 22, no. 5, pp. 1137–1144, 1979, doi: 10.13031/2013.35169.
[46] G. Singh, P. P. Singh, P. P. S. Lubana, and K. G. Singh, "Formulation and validation of a mathematical model of the microclimate of a greenhouse," *Renew. Energy*, vol. 31, no. 10, pp. 1541–1560, Aug. 2006, doi: 10.1016/j.renene.2005.07.011.
[47] R. Gupta, G. N. Tiwari, A. Kumar, and Y. Gupta, "Calculation of total solar fraction for different orientation of greenhouse using 3D-shadow analysis in auto-CAD," *Energy Buildings*, vol. 47, pp. 27–34, Apr. 2012, doi: 10.1016/j.enbuild.2011.11.010.
[48] R. K. Sahdev, M. Kumar, and A. K. Dhingra, "A comprehensive review of greenhouse shapes and its applications," *Frontiers Energy*, vol. 13, no. 3, pp. 427–438, Sep. 2019, doi: 10.1007/s11708-017-0464-8.
[49] A. Papasolomontos, *Good Agricultural Practices for Greenhouse Vegetable Crops Principles for Mediterranean Climate Areas*. Rome, Italy: Food and Agriculture Organization of the United Nations, 2013.

BAHRAM MAHJOOB KARAMBASTI received the B.S. degree in mechanical engineering from Razi University, Iran, in 2009, and the M.S. degree in mechanical engineering–energy conversion from the University of Guilan, Iran, in 2013. His research interests include energy generation, solar energy, multi-objective optimization techniques, CFD, nanofluids, and small-scale power-water production. He is currently working on the efficient use of solar radiation in greenhouse industry for minimizing the energy consumption problem in this sector.

MOHAMAD NAGHASHZADEGAN received the B.S. degree in mechanical engineering from the Iran University of Science and Technology, the M.S. degree in mechanical engineering from the University of Saskatchewan, and the Ph.D. degree in mechanical engineering from The University of Sheffield, U.K., in 1998. He is a Senior Lecturer with the Faculty of Mechanical Engineering, University of Guilan, Iran. His research interests include heat and mass transfer, fluid mechanics, renewable energy, water distribution systems, biofuels, HVAC systems, and CFD.

MARYAM GHODRAT is a Senior Lecturer with the School of Engineering and Information Technology, University of New South Wales (UNSW). Her expertise is in the application of fluid mechanics theories to solve problems related to dynamic behaviour of turbulent multi-phase flows. Her research interests include developing effective numerical tools for practical applications to support mitigating the impact of natural disasters. She is also working in the field of energy efficiency technologies with focus on the application of numerical modeling and thermodynamic analysis in development of new processes.

GHADIR GHORBANI received the B.S. degree in mechanical engineering from the Power and Water University of Technology, Iran, in 2012, and the M.S. degree in mechanical engineering from the K. N. Toosi University of Technology, Iran, 2015. He is currently pursuing the Ph.D. degree in mechanical engineering with Razi University, Iran. Currently, he is working on the novel power-water coproduction systems powered by biofuel and integrated with the solar desalination systems. His research interests include heat and mass transfer, power and water cogeneration power plants, solar energy, and optimization algorithms.

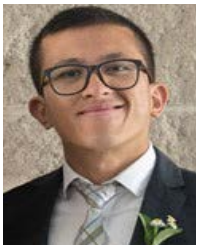

ROY B. V. B. SIMORANGKIR (Member, IEEE) received the B.S. degree in telecommunication engineering from the Bandung Institute of Technology, Indonesia, in 2010, the M.S. degree in electrical and electronic engineering from Yonsei University, South Korea, in 2014, and the Ph.D. degree in electronic engineering from Macquarie University, Australia, in 2018. In 2017, one of his works won first place in the IEEE Region 10 Student Paper Contest, postgraduate category; and was selected as a finalist in the Student Paper and Advanced Practice Paper Competitions of the IEEE MTT-S International Microwave Symposium (IMS), Honolulu. He was the Session Chair of the 2018 ACES Symposium, Beijing. He has been serving as a topic editor for these two journals, and regularly reviews for several reputable journals in his research field. He is currently serving as a Guest Editor of a special issue of *Sensors* journal (MDPI) and *Electronics* journal (MDPI).

ALI LALBAKHSH (Senior Member, IEEE) received the Master of Research (H.D.) and Ph.D. degrees in electronics engineering from Macquarie University, Australia, in 2015 and 2020, respectively. He holds an academic position (Macquarie University Research Fellowship) with Macquarie University. He has published over 110 peer-reviewed journals and conference papers. His research interests include high-gain and flexible antennas, metasurfaces, evolutionary optimization methods, and passive microwave components. He received several prestigious awards, including full scholarships for master's and Ph.D., the Commonwealth Scientific and Industrial Research Organization (CSIRO) grants on Astronomy and Space Exploration; the Macquarie University Postgraduate Research Fund (PGRF); and the WiMed Travel Support Grants. He was a recipient of the 2016 ICEAA-IEEE APWC Cash Prize and the Macquarie University Deputy Vice-Chancellor Commendation, in 2017. He is the only Researcher in the IEEE Region Ten (Asia–Pacific) who received the Most Prestigious Best Paper Contest of the IEEE Region Ten more than once (2016, 2018, and 2019). He was the highly commended finalist in the Excellence in Higher Degree Research Award in Science, Technology, Engineering, Mathematics and Medicine (STEMM) from Macquarie University, in 2019 and 2021. In 2020, he was announced as an Outstanding Reviewer of IEEE TRANSACTIONS ON ANTENNAS AND PROPAGATION and received the Research Excellence Award of the Faculty of Science and Engineering, Macquarie University. In 2021, he received the Faculty Early Career Research Excellence Award and was named one of the Fresh Scientists of New South Wales, Australia. He was also highly commended finalist in the Macquarie University Vice-Chancellor's Learning and Teaching Award. He serves as an Associate Editor for the *International Journal of Electronics and Communications* (AEÜ) and *Electronics* (MDPI).